Since the length of the reflected path and the direct path is essentially the same (differing by only a few wavelengths or less), the amplitude of the two rays due to spatial attenuation (path length) is the assumed to be the same. The reflected ray, however, is multiplied by the reflection coefficient as given above and then shifted (retarded) in phase as a result of the longer path length compared to the direct ray. The vector addition of the two rays at the receiver is thus:

$$E_r = E_d \sin(\omega t) + E_d R \sin(\omega t + \Delta\varphi) \qquad \text{[Eq. 22]}$$

where:

E_d is the magnitude of the direct ray
ω is the carrier frequency in radians
R is the complex reflection coefficient given above
$\Delta\varphi$ is the phase delay of reflected ray in radians

The carrier term is usually suppressed so that [Eq. 22] becomes:

$$E_r = E_d\left(1 + |R|\angle(\varphi_r + \Delta\varphi)\right) \qquad \text{[Eq, 23]}$$

where φ_r is the phase angle of the reflection coefficient. The term $\Delta\varphi$ is found from the actual path length difference in meters. For a two-ray path geometry over a curved earth, the path length difference as given by (5.9) in [15] as:

$$\Delta r = \frac{2h_t' h_r'}{d_r} \qquad \text{[Eq. 24]}$$

where:

h_t' is the height of the transmit antenna *above the reflecting plane* in meters
h_r' is the height of the receive antenna *above the reflecting plane* in meters

so that:

$$\Delta\varphi = \frac{2\pi\Delta r}{\lambda} \quad \text{(modulo } 2\pi \text{ radians)} \qquad \text{[Eq. 25]}$$

The usual issue in using this approach is defining where the reflecting plane is for a complex terrain profile between the transmitter and receiver.

For the Anderson 2D model the reflection point is found by evaluating the angle of incidence and reflection at every terrain elevation point between the transmitter and receiver. The angle of incidence at any point along the profile (the evaluation point) is found from simple geometry as follows:

$$\gamma_t = \tan^{-1}[(h_t / d_t] \qquad \text{[Eq. 26]}$$

for the transmitter, and

$$\gamma_r = \tan^{-1}[(h_r / d_r] \qquad \text{[Eq. 27]}$$

for the receiver. The terms h_t, h_r, d_t, and d_r are the transmitter height above the evaluation point, the receive antenna height above the evaluation point, and the distances for the evaluation point to the transmitter and receiver, respectively. The evaluation point where $\gamma_t = \gamma_r$ is considered the reflection point. However, it is unlikely that these angles with ever be exactly equal. In such cases, at the two adjacent evaluation points where the angles inflect (i.e. γ_r becomes larger than γ_t), the reflection point is considered to exist along the profile segment defined by the adjacent points. The exact reflection point is then found along this profile segment using linear interpolation since the profile segment is by definition a linear slope. With the distance and elevation of the reflection point established, the reflection angle of incidence γ_0 is found using an equation of the form of [Eq. 25]. This value of γ_0 is then used in [Eq. 18] and [Eq. 19] to find the magnitude and phase of the reflection coefficients.

The effect of the nearby ground reflection will be to reduce the amplitude of the directly received ray because in general they will add out of phase and the amplitude of the reflected ray will be nearly equal to the direct ray because at low reflection angles of incidence, $|R| \cong 1.0$ for most practical combinations of frequency, conductivity, and permittivity. For an antenna placed very near the ground, the cancellation based on these formulas will be almost perfect so that the direct received (free space) ray will be reduced by 40 dB or more. However, it is unlikely that such a perfect cancellation will occur, therefore it is appropriate to put some reasonable limits on the change in the amplitude of the directly-received ray which can occur due to a reflection. Based upon measurement and theoretical data, the limits on the change in the free space amplitude due the reflection contributions will be -25 dB and + 6 dB.

Thus based on the preceding discussing, the path loss or attenuation term $A_{reflection}$ can be written as:

$$A_{reflection} = 20.0 \log \left[\left(1 + |R| \angle (\varphi_r + \Delta\varphi) \right) \right] \text{ dB} \qquad \text{[Eq. 28]}$$

with the limits that $-6.0 \text{ dB} \leq A_{reflection} \leq 25.0 \text{ dB}$.

5.2.2.2 Attenuation Due to Partial Obstruction of the Fresnel Zone

When a path is LOS but terrain obstacles are close to obstructing the path, additional attenuation will occur which cannot be accounted for using the ray approach from

geometric optics. This is because the geometric optics only deals with energy transport, not phase. As such, the frequency is infinite and the wavelength is zero. With zero wavelength, the Fresnel zone radius is also zero. The failure of the ray approach to account for attenuation due to a "near miss" of obstacles on the path can be overcome to some extent by including a loss term in the LOS formulation which is based on the extent to which an obstacle penetrates the first Fresnel zone. From diffraction theory, when the ray just grazes an obstacle, the field on the other side is reduced by 6 dB (half the wavefront is obstructed). When the clearance between the obstacle and the ray path is 0.6 of the first Fresnel zone, the change in the field strength at the receiver is 0 dB, and with additional clearance a field strength increase of 6 dB can occur owing to the in-phase contribution from the ray diffracted from the obstacle. For additional clearance, an oscillatory pattern in the field strength occurs, as conveniently illustrated by Figure 7.1 in [15].

For the Anderson 2D model, if the ray path clears intervening obstacles by at least 0.6 of the first Fresnel zone, then no adjustment to the receiver field will occur. For the case when an obstacle extends into the 0.6 first Fresnel zone, a loss factor ranging from 0 to 6 dB will be applied based on a linear proportion of how much of the 0.6 First Fresnel zone is penetrated. This Fresnel zone path loss or attenuation term can be written as:

$$A_{Fresnel} = 6.0\left(\frac{C_{obs}(d_p)}{R_{FR}(d_p)}\right) \text{ dB} \qquad \text{[Eq. 29]}$$

where:

$C_{obs}(d_p)$ is the height difference in meters between the ray path and the terrain elevation at distance d_p along the path

$R_{FR}(d_p)$ is the 0.6 first Fresnel zone radius at distance d_p along the path

The values $C_{obs}(d_p)$ and $R_{FR}(d_p)$ are calculated taking into account the effective earth radius using the K factor. The 0.6 first Fresnel zone radius is given by:

$$R_{FR}(d_p) = 0.6\left[549.367\sqrt{\frac{d_p(d_r - d_p)}{f\,d_r}}\right] \text{ meters} \qquad \text{[Eq. 30]}$$

where f is the frequency in MHz and all distances are in kilometers.

The use of the partial Fresnel zone obstruction loss from 0 dB at 0.6 clearance to 6 dB at grazing also provides a smooth transition into the NLOS mode in which knife-edge diffraction loss just below grazing will start at 6 dB and increase for steeper ray bending angles to receive locations in the shadowed region. Note that this attenuation factor is found only for the terrain profile point which extends farthest into the 0.6 first Fresnel zone, not for every profile point which extends into the Fresnel zone.

5.2.2.3 Summary of the Calculation of the Field Strength at the Receiver Under LOS Conditions

All of the formulations for computing the field strength at the receiver under LOS conditions are now in place. They can be summarized with the following simple equation:

$$E_r = 76.92 - 20\log(d_r) + P_T - A_{reflection} - A_{Fresnel} - A_{clutter} \text{ dBuV / m} \qquad \text{[Eq. 31]}$$

where $A_{reflection}$ is the change due the reflection in dB from [Eq. 28], $A_{Fresnel}$ is the partial Fresnel zone obstruction loss from [Eq. 29]. $A_{clutter}$ is a local clutter loss number which will range from 0 dB to 17 dB as discussed in Section 5.4 and as shown in Table 12. The term P_T is the effective radiated power (ERP_d) in dBW in the direction of the receiver.

In terms of path loss between two antennas with gains of 0 dBi in the path direction, [Eq. 31] can be written as:

$$L_{LOS} = 32.45 + 20.0\log f + 20\log d_r + A_{reflection} + A_{Fresnel} + A_{clutter} \quad \text{dB} \quad \text{[Eq. 32]}$$

5.2.3 Non-Line-of-Sight (NLOS) Mode

The decision on when to use the LOS mode and when to use the NLOS modes was set forth at the beginning of Section 5.2.2. If the model has elected to use the NLOS formulations, it means that one or more terrain or other features obstructs the ray path directly from the transmitter to the receiver. In this case, the free space field strength is further reduced for the attenuation cause by the obstacles. For the model defined here, the calculation of obstruction loss over an obstacle will be done by assuming the obstacle is a perfect electrical conductor (PEC) rounded obstacle with a height equal to the elevation of the obstruction and a radius equal to 1 meter. Diffraction loss in this model is calculated assuming individual obstacles on the path can be modeled as isolated rounded obstacles. The loss from each isolated obstacle is then combined using the Epstein-Peterson technique [10] as extended to more than two obstacles. The NLOS mode also include loss for partial Fresnel zone obstruction due to sub-path obstacles along the path from the transmitter to the first obstacle and from the last obstacle to the receiver. This partial Fresnel zone obstruction losses are found exactly as described in Section 5.2.2.2.

5.2.3.1 Diffraction Loss

The loss over an individual rounded obstacle is computed using the formulas taken from [1]. It is primarily a function of the parameter ν which is related to the path clearance over the obstacle. The total diffraction loss, $A(\nu,\rho)$, in dB is the sum of three parts $-A(\nu,0), A(0,\rho)$, and $U(\nu,\rho)$ The equations to calculate each part are given below:

$$A(\nu,\rho) = A(\nu,0) + A(0,\rho) + U(\nu,\rho) \qquad \text{[Eq. 33]}$$

$$A(v,0) = 6.02 + 9.0v + 1.65v^2 \quad \text{for } -0.8 \le v \le 0 \qquad \text{[Eq. 34]}$$

$$A(v,0) = 6.02 + 9.11v - 1.27v^2 \quad \text{for } 0 < v \le 2.4 \qquad \text{[Eq. 35]}$$

$$A(v,0) = 12.953 + 20\log_{10}(v) \quad \text{for } v > 2.4 \qquad \text{[Eq. 36]}$$

$$A(0,\rho) = 6.02 + 5.556\rho + 3.418\rho^2 + 0.256\rho^3 \qquad \text{[Eq. 37]}$$

$$U(v,\rho) = 11.45v\rho + 2.19(v\rho)^2 - 0.206(v\rho)^3 - 6.02 \text{ for } v\rho \le 3 \qquad \text{[Eq. 38]}$$

$$U(v,\rho) = 13.47v\rho + 1.058(v\rho)^2 - 0.048(v\rho)^3 - 6.02 \quad \text{for } 3 < v\rho \le 5 \qquad \text{[Eq. 39]}$$

$$U(v,\rho) = 20v\rho - 18.2 \quad \text{for } v\rho > 5 \qquad \text{[Eq. 40]}$$

where the curvature factor is:

$$\rho = 0.676R^{0.333} f^{-0.1667} \sqrt{\frac{d}{d_1 d_2}} \qquad \text{[Eq. 41]}$$

The obstacle radius R is in *kilometers*, and the frequency f is in MHz. The distance term d is the path length from the transmitter (or preceding obstacle) to the receiver (or next obstacle), d_1 is the distance from the transmitter (or preceding obstacle) to the obstacle, and d_2 is the distance from the obstacle to the receiver (or next obstacle). When the radius is zero, the obstacle is a knife edge and $A(v,\rho) = A(v,0)$.

The parameter v in the above equations takes into account the geometry of the path and can be thought of as the bending angle of the radio path over the obstacle. It is computed as:

$$v = \sqrt{\frac{2d\tan(\alpha)\tan(\beta)}{\lambda}} \qquad \text{[Eq. 42]}$$

where d is the path length from the transmitter (or preceding obstacle) to the receiver (or next obstacle), α is the angle relative to a line from the transmitter (or preceding obstacle) to the receiver (or next obstacle), and β is the angle relative to a line from the receiver (or next obstacle) to the transmitter (or preceding obstacle). The definition of α and β are shown if Figure 8. For the multiple obstacle case, obstacles are treated successively as transmitter-obstacle-receiver triads to construct the path geometry and bending angle v over each obstacle. The value of v is then used to calculate the diffraction loss over each obstacle. The resulting obstacle losses are summed to arrive at the total obstacle diffraction loss for the path.

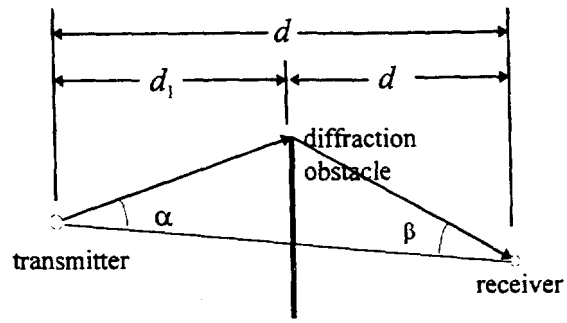

Figure 8. Geometry for computing ν

5.2.3.2 Handling Anomalous Terrain Profiles

Experience with terrain elevation databases covering the United States has shown that occasional anomalous profiles can be produced. A typical example is a "false" plateau in which the several adjacent data points all have the same or nearly the same value, and that value is usually exactly equal to a contour elevation line (like 400 or 600 feet) on the original 1:250,000 scale maps from which the original database was developed. Under LOS conditions these plateaus are usually not a problem but if they form an obstruction to the ray between the transmitter and the receiver, using the Epstein-Peterson type geometry, it may occur that every point on the top of the plateau appears to be an obstacle. The result is a string of diffracting points, many with grazing incidence, and a predicted diffraction attenuation in excess of what would actually occur. The following method is included in the Anderson 2D model for detecting and dealing with such anomalies.

When the model finds more that two consecutive points along the terrain profiles are obstacles using the geometry described above, it ignores all the intermediate obstacles. Instead, it preserves the obstacles at the beginning and at the end of the sequence as two rounded obstacles with a radius of 1 meter and calculates the diffraction loss over each as described above. In urban ray-tracing models, using this two-edge diffraction approach is common for computing ray attenuation over real plateau-like features such as buildings, provided slope diffraction coefficients are used at the second edge. For terrain profiles, this approach provides a simple way of resolving the anomalies which will also be approximately correct for real plateau obstacle features along the path.

5.2.3.3 Summary of the Calculation of the Field Strength at the Receiver Under NLOS Conditions

The field strength at the receiver in the NLOS mode can then be written as:

$$E_r = 104.77 - 20\log(d_r) + P_T - A_{diff} - A_{T,Fresnel} - A_{R,Fresnel} - A_{clutter} \text{ dBuV / m} \quad \text{[Eq. 43]}$$

where all the terms have the same definitions as given in Section 5.2.2.3 and the term A_{diff} is defined as:

$$A_{diff} = \sum_{n=1}^{NOBS} A_n(\nu,\rho) \quad \text{dB} \qquad \text{[Eq. 44]}$$

where $A(\nu,\rho)$ is defined in [Eq. 33]. The terms $A_{T,Fresnel}$ and $A_{R,Fresnel}$ are the partial Fresnel zone obstruction attenuations on the path segments from the transmitter to the first obstacle, and from the last obstacle to the receiver, respectively, as described above.

The corresponding path loss between antennas with 0 dBi gain in the path direction can be written as

$$L_{NLOS} = 32.45 + 20.0\log f + 20\log d_r + A_{diff} + A_{T,Fresnel} + A_{R,Fresnel} + A_{clutter} \quad \text{dB} \qquad \text{[Eq. 45]}$$

5.3 Terrain Elevation Database

The propagation prediction model defined in this specification inherently depends on the terrain database to compute the effective base antenna height for use in Section 5.1 and for the geometry computations for the shadow loss formulations in Section 5.2. In the United States, there are currently three terrain databases which are commonly used:

1. The 30 arc second National Geophysical Data Center (NGDC) database

2. The 3 arc second (U.S. Geological Survey (USGS) or Defense Mapping Agency (DMA)) database

3. The 30 meter (USGS) database

The 30 second database is primarily used by the FCC and those filing FCC applications to determine 2-10 miles (3-16 km) average terrain along radials emanating from a transmitter site for the purpose of determining the location of coverage of interference signal contours. Because of its wide point spacing (nearly 1 km), its use for more detailed propagation studies is not common.

The 3 arc second database is the one most commonly used for propagation studies. Its point spacing of about 90 meters north-south by an average point 70 meters east-west seems appropriate for many planning purposes, especially when wide-area systems with service radii of 50 km or more are being considered. Considering coverage and interference on a grid with spacings less than 100 meters is rarely necessary. The 3 arc second database is also a convenient size for use on personal computers since with reasonable compression techniques the entire database can fit and be used from an inexpensive CD-ROM drive.

The main drawback to the 3 arc second database is its vertical accuracy. For the most part it was derived from the 1:250,000 series of maps covering the US. Most of these maps have contour intervals of 200 feet. The result is that many ridges and hills with peak elevations that lie between 200 foot contour intervals are not properly represented. Even some peaks where USGS benchmarks are shown on the maps were not properly digitized. Occasionally, elevation errors occur, some as great as 200 meters.

The 30 meter data contains elevation data points spaced at 30 meter intervals rather than intervals based on latitude and longitude. Its development has been a on-going effort by the USGS over the last several years. It is fundamentally derived using contour and other information from the 7.5 minute quadrangle series maps which cover the US. Since the data source is a much larger scale the data source for the 3 second database, the vertical accuracy achieved is significantly better. Unfortunately, at this time the data files for only slightly more than 60% of the USA have been completed and released. New data files are released on a monthly basis.

Despite these uncertainties, the much improved vertical accuracy of the 30 meter data warrants consideration for a development effort of an up-to-date propagation model. With incomplete coverage, some techniques will need to be developed to handle transitions from the 30 meter data to the 3 second data which does cover the entire country. Smoothing individual terrain profiles at the transition is one possibility. Another, much more extensive, approach is to meld or re-grid the 30 meter data into the existing 3 second format. The net result of this effort would be a database with 3 second point spacings (sufficiently close as explained above) but with the improved vertical accuracy of the 30 meter data. Re-gridding data in this way is computationally extensive but straightforward. It is similar to the effort required when developing a terrain elevation database from information which has been digitized from a topographic map. The raw digitized data consists of a collections of flat lines, slope lines, and points. By considering all this information together, a smooth, internally consistent set of Digital Elevation Model (DEM) matrices can be produce with essentially arbitrary grid point spacings.

Because of its nationwide coverage, for the model defined here, the 3 arc second database will be the fundamental terrain database used. Where 30 meter data is available, its use is preferred. The calculation results based on the use of 30 meter data *along the entire transmitter-receiver path* shall take precedence over the those based on the 3 arc second data when there is a dispute about model prediction results.

5.3.1 Establishing Terrain Elevation Points Along a Profile Using the Terrain Database

In practice the model requires a terrain elevation profile to be defined between the transmitter and the receiver. This profile is fundamental to the path loss prediction techniques in Sections 5.1 and 5.2. The elevation points on this profile are to be extracted from the terrain database by first determining the great circle path from the transmitter to the receiver. Spacing between adjacent data points shall not exceed 0.2 km or 0.2% of the

path length, whichever is less. Either method can be used regardless of the horizontal resolution of the database. Either of the following extraction techniques is acceptable.

5.3.1.1 Bilinear Interpolation

A profile elevation point spacing is selected. At a point some distance *d* from the transmitter along the great circle path where the profile elevation is to be found, the latitude-longitude or other coordinates of the point (the lookup point) are determined using double precision spherical trigonometry. These coordinates are then used to find the four surrounding elevation points; linear interpolation is used to establish the elevation at the lookup point. This process is used to find the elevation at each of the points along the profile from the transmitter to the receiver.

5.3.1.2 "Snap to Nearest Point" Method

The equation of the line segment between the transmitter and the receiver is established. Using conventional spherical trigonometry techniques, the distances from all points to the line are determined. The elevations of all points within 0.5x (the horizontal resolution of the database) are used. Their corresponding horizontal positions along the profile are the crossing points of perpendiculars from the points to the line. This method produces profiles with unequal horizontal spacings, but the results produce equally valid results as those using the method described above.

5.4 Local Clutter Loss Attenuation Standard Values

The path loss predictions in Sections 5.1 and 5.2 can be improved by applying a local clutter loss factor. Whether an urban, suburban, or foliage loss should be applied is determined by a land use or groundcover type associated with the receiver location. The land use/land cover (LULC) database which is currently available for the US comes from the USGS. It is actually available in two forms - as vector data describing the boundaries of land use region types, and as composite theme grids (CTG) files in which 1 of 37 land use types have been assigned to 200 meter square grid cells covering the entire country. The CTG files are the ones which are generally used with propagation models.

This database also has shortcomings. Much of the information was taken from 1:250,000 scale maps which limits its resolution. It also can be rapidly dated as new construction turns farms into subdivisions and factories. But at this time, the USGS LULC database is the only one that is readily available and for that reason, it is specified that it be used in this model for the purpose of determining the local clutter classification at each receive point. If a new database, or better database information becomes available through LandSat or other sources, then that better data can supersede the LULC data.

With the exception of categories 11-17, the remaining land use classifications in the LULC database are much too fine-grained for radio propagation use. Table 11 shows a recommended way of reducing the 37 classifications to 10. Table 12 shows the value of $A_{clutter}$ to be used for each of the reduced classifications as a function of frequency. For frequencies not shown in the table, linear interpolation in dB is to be used between the

values shown in the table. To use the values in Table 12 with the programs in Section 5.1.2, the "open" mobile environment must be chosen. Choosing other mobile environments will result in predictions showing signals weaker than actual.

5.5 The Anderson 3D Propagation Methods for Time Dispersion and Multipath Predictions

It is well know that in hilly and mountainous areas reflections from terrain features can cause signal echoes to arrive at the receiver some time after the signal received directly from the transmitter. If the directly-received signal is weak due to shadowing, these reflections can actually be of comparable or higher amplitude than the directly-received signal. Such multipath effects are commonly recognized as "ghosting" in broadcast television. Depending on the data rate, for some types of digital transmission systems in mobile communications these echoes can have an important effect on bit error rate (BER) performance of the system [16].

The prediction of multipath time dispersion from terrain features is a relatively new field of research. As will be discussed, many specific parameters controlling the performance of the model cannot yet be established with the limited amount of field measurement data which is available. Therefore, the intent of this section is to outline an approach to prediction multipath time dispersion in a 3D terrain environment with sufficient detail that others can reproduce the method if desired. No equations are provided here.

The method described here can be viewed as an extension of the 2D transmitter-receiver path profile path loss prediction analysis set forth in Sections 5.1 and 5.2.

The first step in the method is to determine the terrain surrounding the base station which is illuminated by the base station. This can be done by finding the terrain elevations in a grid surrounding the base station out to distance beyond that where the signal dispersion is actually required. This is because terrain features beyond the coverage area of interest may reflect back into the area of interest. An initial test value considers terrain at distances 50% greater than the service area distance of interest.

Within this grid area, elevation points are extracted from the database at 0.5 or 1 km intervals. The four corner elevation points form a square through which a plane can approximately be constructed using standard analytical geometry. The vector normal to the plane defines its orientation. The normal to the plane is found as the cross product of any two vectors in the plane. The vectors can be those connecting two of the corner grid points, for example, if they lie on the plane. The normal vector is resolved in to x,y,z components. The ratio of the z component to the overall magnitude of the normal vector is inversely proportional to the slope of the plane. The first sorting process after constructing the terrain grid is to evaluate the magnitude of the slope for each plane and determine whether it has sufficiently slope to be further considered as a reflecting source. The threshold for such consideration has not yet been established.

For those planes or patches which have sufficient slope, the next step is to find the angle between the normal vector and the vector from the patch back to the base station. If the angle of this vector is less that 90 degrees, the patch is oriented such that it is illuminated to some degree. Angles greater than 90 degrees indicate the patch is oriented away from the base station and will not be illuminated. As a practical matter, the difference angle should be substantially less than 90 degrees so that the patch has sufficient cross-sectional area to intercept and reflect a relevant amount of energy.

At this point all the patches have been sorted so that only those with sufficient slope and which "face" the transmitter are still considered. For each of these patches a terrain profile is constructed from the transmitter to the center of the patch to determine whether it is line-of-sight (LOS) or shadowed. If it is shadowed, it is excluded from further consideration since it probably won't have a strong enough incident field strength to produce important reflections. In mountainous areas with sheer rock faces, however, this assumption is probably not valid.

All the LOS patches determined to this point are illuminated by the base station. The next step is to considered each receive location in a grid or other study configuration, and at each such point, determine if the geometry of reflection is such that a reflected signal will illuminate the receiver. This is done using the vector from the patch to the base station, the vector from the patch to the receive location, and the vector normal to the patch. If the geometry is such that a reflection could be important, then the final step is to find the terrain profile from the patch to the receiver to see if it is LOS. If is shadowed, it will be assumed (as above) that the reflection will not be important at the receiver. If it is LOS, than the reflected signal amplitude can be found at the receiver. Some available empirical data by Dreissen [11] suggest that the return loss on the reflection is on the order of 20 to 30 dB. Therefore, a first estimate of the reflected signal amplitude at the receiver would be the amplitude the signal would have had given an LOS path of equivalent transmitter-reflector-receiver length, but reduced by 20 to 30 dB. The reflected echo transit time is easily found using the total transmitter-reflector-receiver path length. The time delay of the echo is this time minus the time for the directly received signal to arrive given its (shortest) path length.

Using the reflected echo amplitudes and time delays, a power delay profile can be constructed and the RMS delay spread determined (Section 6.7). The RMS delay spread can then be used to estimate BER values for various digital systems.

The mechanics of the described method have been implemented in a software model. An ensemble of multipath echoes at the received occur as expected. However, to breathe real life into the model, all those places in the model description where words like "substantial" and "significant" need to be replaced by quantifiable thresholds. Further development of the model will be directly toward establishing these thresholds.

A similar technique for 3D terrain scattering for radio propagation prediction purposes, including mathematical details, can be found in reference [12].

5.6 Propagation Modeling and Simulation Benchmarks

The following referenced path profiles and tabulated path losses are to serve as benchmark results of the propagation prediction model. Those interested in creating computer implementations of the model described in this section can use these tests to verify their implementation.

From the NBS measurement program reported by McQuate *et al* [17] and studies by Hufford [20], path numbers:

R1-20-T1	R2-10-T3	T1-10-R1
R1-20-T3	R2-10-T4	T1-10-R3
R1-20-T7	R2-10-T7	T1-10-R6
R1-50-T4	R2-20-T5	T1-20-R5
R1-50-T5	R2-20-T8	T1-80-R7
R1-50-T6	R2-20-T9o	T4-50-R7
R1-50-T7	R2-50-T3	T5-20-R7
R1-50-T8	R2-50-T4	T6-10-R2
R1-50-T9	R2-50-T5o	T7-80-R6o
R1-80-T1	R2-120-T2	
R1-120-T5	T1-5-R1	

The exact endpoint coordinates for these paths are contained in [17] [20]. Measured path loss as a function of receive antenna height above ground and at several frequencies are shown on graphs in [17] [20].

Because the paths in [17] [20] are for antenna heights relatively low to the ground, and no over-water nor desert paths are involved, a few additional paths are included for the model benchmark. Five paths start from Mt. San Bruno (North latitude 37° 44' 22", West 122° 26' 10") south of San Francisco where several transmit facilities on different frequencies are in operation. The model benchmark paths from Mt. San Bruno are azimuths 0, 45, 90, 135, and 180 degrees out to a distance of 50 km. Measured path loss data at different frequencies are not yet available for the Mt. San Bruno paths.

Two paths start from Onyx Peak (North latitude 34° 11' 31", West longitude 116° 42' 29" elevation 2778 m AMSL) east of Los Angeles, where several transmit facilities on different frequencies are in operation. The model benchmark paths are azimuths 41 and 95 degrees out to a distance of 90 km. Measured path loss data at different frequencies are not yet available for the Onyx Peak paths.

5.7 Recommendations Concerning Tiled vs. Radial Metaphors

A number of possibilities exist for defining the plane of the service area. The most widely used are the following:

- The Radial method
- The Stepped Radial method
- The Grid Mapped from Radial Data method
- The Tiled Method

5.7.1 Radial Method

In the radial method, many radials are drawn at equal angular intervals from the site to the far edge of the service area. Elevation points are extracted from the database at intervals along each radial. Each point represents an annular segment of service area. Since the radials get farther and farther apart as the distance from the site increases, care must be taken to ensure that the number of radials is sufficient to adequately characterize the area near the outer edge.

5.7.2 Stepped Radial Method

In the stepped radial method, the angular interval is stepped with distance. For example, in the CSPM [13] method, 8 radials are drawn from 0 to 2 km, 16 radials for 2 to 4 km, and so on up to 2,048 radials at distances of greater than 128 km. This results in a distance between radial ends not exceeding 1.57 km for all distances up to 256 km. Once again, each point along a radial represents an annular segment.

5.7.3 Grid Mapped from Radial Data Method

With this method, basic path loss information is calculated at points along radials as described in Section 5.7.1 or 5.7.2, and this information is then mapped into a uniform grid using linear or other interpolation methods. The derived signal levels at the grid locations can be then used for analyzing signals from multiple transmitters at common locations. This method combines the calculation speed advantages of radial methods over tiled methods, while still providing a common grid or tile structure for uniform multi-transmitter system analysis.

5.7.4 Tiled Method

In the tiled method, rectangular[2] tiles of a given size are predefined throughout the service area. Radials are drawn to each of these tiles. This results in unequal angular spacing and a greater number of required radials to predict signal levels in a given geographical area. The advantage is that a specific path loss calculation has been done to each tile centroid rather then being interpolated from nearby path loss calculation points.

5.7.5 Discussion of Methods

In predicting signal strength, only the radial method presents any kind of problem and, if the user is willing to increase the number of radials sufficiently, that problem can be averted. In predicting interference or simulcast performance, however, new problems arise. In the tiled method, all predictions from all sites are done to the same set of endpoints.

---

[2] In practice, the tiles may be squares or curvilinear trapezoids as well.

Therefore, signal strength and delay spread prediction values can be calculated at those points. The grid mapped from radial data method provides a similar feature by using a set of interpolated endpoints.

Conversely, however, either radial method predicts to arbitrary endpoints. For a two-site system, the situation is not hopeless. The program must calculate the crossing points between the radials originating at the two sites and calculate its capture ratios, signal strengths, and delay spreads at those points. However, radial crossings become extremely far apart at angles approximating the azimuth between the two sites. Overall, the results of the radial approach to simulcast or interference prediction in a two-site system are mediocre at best.

In a system of three or more sites, the problem becomes more complicated. The tiled method still works well because the calculation points are predefined. The grid mapped from radial method also does the job. The radial method, however, becomes even more problematic. It is highly improbable that there will be ANY crossings that exist between radials from three or more sites. This means that any straight radial system cannot be used.

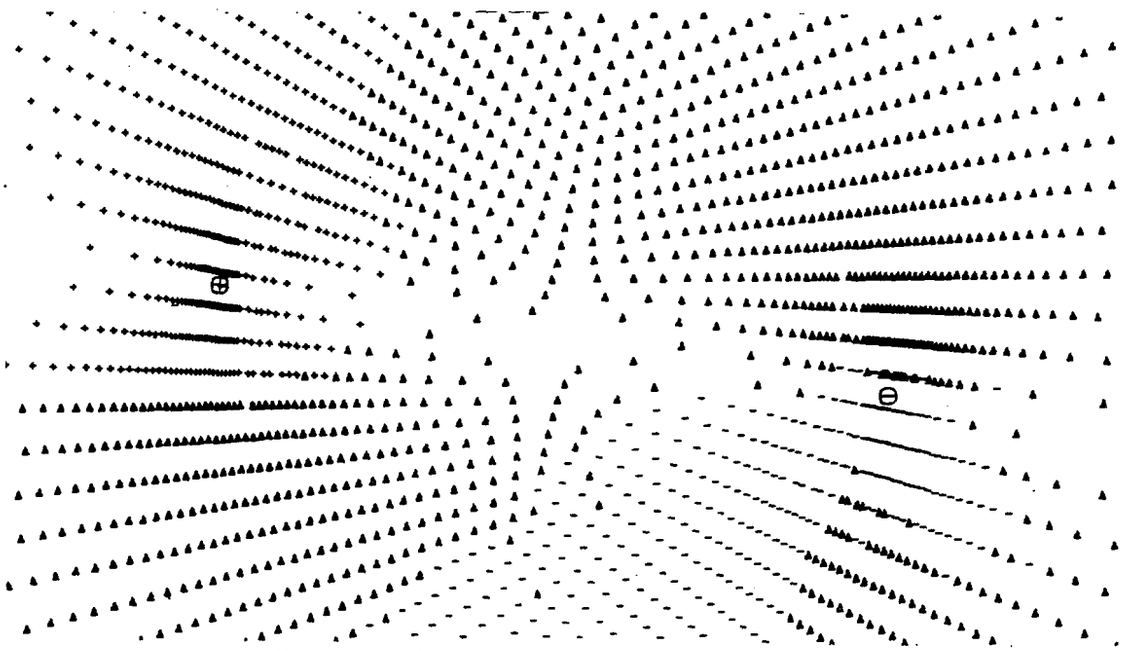

Figure 9. Radial Crossings in a 2-Site System

Notes to Figure 9:
Note 1: Figure is a randomly-selected capture ratio map
Note 2: Symbols:
Circled "+" = Site 1
"+" = Signals from Site 1 exceed those from Site 2 by predetermined ratio
Circled "-" = Site 2
"-" = Signals from Site 2 exceed those from Site 1 by predetermined ratio
"▲" = Capture ratio does not exceed predetermined value
Note 3: In the example, the "+" site is omni and the "-" is directional toward 240°

5.7.6 Summary and Recommendations

All four of the methods listed above can provide acceptable results for predicting signal strengths in the region around a single transmitter if proper consideration is given to the resolution of the study method and the objectives of the signal strength prediction. However, for simulcast, interference, best server, and other studies involving two or more transmitters, of the four methods listed, the grid mapped from radial method (Section 5.7.3) and the tiled method (Section 5.7.4) are best suited to providing acceptable results and are therefore recommended for such applications.

5.8 Reliability Prediction

The prediction of mean signal strength at a given location can vary from the measured signal for many reasons, including the following:

- Prediction algorithm not adequate
- Terrain database imperfections
- Land cover database imperfections
- Measurement made at slightly different location than prediction

Because of this, the signal at any one location can vary from that predicted by the model. It is recommended that a 1 dB margin be added for these "uncertainty" effects.

Additionally, signal variations due to land clutter tend to follow a lognormal distribution with a standard deviation of 5.6 dB. This value is applicable only when the terrain database recommendations of Section 5.3 are followed, including the local clutter database from Table 11 in Appendix-A and the shadow loss method of Section 5.2. A measurement error with a standard deviation of 1 dB is also included.

In determining the amount of extra margin to include, the user should set a required reliability level, and (because the only interest is in the signal equaling or exceeding a given value, rather than being in a given range) apply the "one-tailed" statistical test. Values of suggested margins for particular predicted reliabilities follow; these values are applicable only when the terrain database recommendations of Section 5.3 are followed:

Service Area Reliability	Clutter Margin	Uncertainty Margin	Total Margin
90 %	7.2 dB	1.0 dB	8.2 dB
95 %	9.2 dB	1.0 dB	10.2 dB
97 %	10.5 dB	1.0 dB	11.5 dB

No additional margin is required for time (temporal reliability). Time is considered to be 100%. This implies that measurements taken at different times over the same locations would produce similar results. Seasonal changes should be evaluated for worst case scenarios, such as trees losses with leaves rather than without.

5.9 Interference Calculations

Two methods of calculating interference from multiple lognormally-distributed sites are presented here: Monte Carlo simulation, and the "Equivalent Interferer" method. The Monte Carlo method can produce a more precise representation for the sum of lognormal interferers. However, for this application, the inherent accuracy of both methods is limited by the accuracy with which the constituent interference distributions are known.

5.9.1 Equivalent Interferer Method

If there is only one potential interferer, use its mean and standard deviation. If there are more than one, calculate the statistics of the "equivalent interferer" as follows:

1. $$\mu_j = 10^{\frac{m_{jdB}}{10}} \times \exp\left(\frac{\sigma_{jdB}\ln(10)}{20}\right)$$ [Eq. 46]

$$D_j^2 = 10^{\frac{m_{jdB}}{5}} \times \left[\exp\left(\frac{\sigma_{jdB}\ln(10)}{5}\right) - \exp\left(\frac{\sigma_{jdB}\ln(10)}{10}\right)\right]$$

2. $$\mu = \sum \mu_j$$ [Eq. 47]

$$D^2 = \sum D_j^2$$

3. $$\sigma_{nat}^2 = \ln\left(\frac{D^2}{\mu^2} + 1\right)$$ [Eq. 48]

4. $$m_{eq(nat)} = \ln(\mu) - \frac{\sigma_{nat}^2}{2}$$ [Eq. 49]

$$m_{eq(dB)} = m_{eq(nat)} \times 10\log_{10}(e)$$

where:

m_{jdB} ≡ The mean signal level of the jth potential interferer in dB
σ_{jdB} ≡ The standard deviation of the jth potential interferer in dB
$m_{eq(dB)}$ ≡ The median strength of the equivalent interferer

Note: Use the same standard deviation for all interferers, except for the background noise level. Use a 0 standard deviation for the background noise.

If SIGN[$\tau/(2s_d)$] ≠ -1, substitute into the following equation:

$$R = 1 - 0.5 erfc\left[\tau / \left(2s_d\right)\right]$$

where:

$\tau = m_d - m_{eq} - C/I_{req}$
i.e., the mean desired - equivalent interferer - required in C/I in dB
s_d = the standard deviation of the desired signal in dB, ***not*** the calculated value in natural units

If SIGN[$\tau/(2s_d)$] = -1, solve for R by substituting the absolute value of $\tau/(2s_d)$ for $\tau/(2s_d)$ in the equation for R, then by subtracting this result from 1.

Example of Equivalent Interferer Method:

Assume the following:

- A proposed analog FM system desiring DAQ-3 coverage.
- At a given location, the desired station has a signal strength of -75 dBm.
- Three potential interferers of -102, -108, and -111 dBm.
- Standard deviation of 5.7 dB.
- Noise for an ENBW of 16 kHz at 150MHz in a residential district.

m_{1dB} = -102	σ_{1dB} = 5.7	μ_1 = 121.6186E-12	D_1^2 = 401.6300E-22
m_{2dB} = -108	σ_{2dB} = 5.7	μ_2 = 30.5492E-12	D_2^2 = 25.3411E-22
m_{3dB} = -111	σ_{3dB} = 5.7	μ_3 = 15.3109E-12	D_3^2 = 6.3654E-22

Calculate m_{4dB}, the noise value, from Section 4.2.

m_{4dB} = -114	σ_{4dB} = 0	μ_4 = 3.9811E-12	D_4^2 = 0

$$\mu = \sum \mu_j = 171.4598E - 12 \qquad D^2 = \sum D_j^2 = 433.3366E - 22$$

$$\sigma_{nat}^2 = \ln\left[\frac{4.333366 \times 10^{-20}}{\left(1.714598 \times 10^{-10}\right)^2} + 1\right] = \ln\left(\frac{4.333366 \times 10^{-20}}{2.939846 \times 10^{-20}} + 1\right) = \ln(2.474011) = 0.9058408$$

$$m_{eq(nat)} = \ln\left(1.714598 \times 10^{-10}\right) - \frac{.90958408}{2} = -22.93959 nats$$

$$m_{eq(dB)} = -22.93959 \times 4.343 = -99.6 dB$$

Substituting into (5.9-2), m_{eq} = -99.6 dB

τ = -75 - (-99.6) - 17 = 7.6

Where -17 is the C/I value corresponding to CM3.

$$R = 1 - 0.5 \times erfc\left(\frac{7.6}{2 \times 5.7}\right)$$
$$= 1 - 0.5 \times .346$$
$$= 0.827$$

5.9.2 Monte Carlo Simulation Method

Treating the remaining sites as potential interferers, run Monte Carlo simulations for points uniformly distributed over the proposed service area. For each point in the proposed service area, do the following in Sections 5.9.2.1 through 5.9.2.6.

5.9.2.1 Calculate Deterministic Signal Strengths

Calculate the (deterministic) signal strengths from the desired station and for all potential interferers at the location currently of interest using the methods of §§ 5.0 - 5.8. The results' should be expressed in dB values (e.g., dBm).

5.9.2.2 Draw from a Pseudorandom Number File

For the proposed station and for all potential interferers, draw a small number of times (e.g., 500) from a pseudorandom number file which has the following distribution: Type = Normal, standard deviation = 1, mean = 0. [For a proposed station and three potential interferers, this will result in 2000 draws, 500 corresponding to each station.]

5.9.2.3 Multiply by Known Standard Deviation

Multiply the values thus found by the known standard deviation for the area under consideration. See Section 5.8.

5.9.2.4 Offset the Calculated Signal Strengths

Offset the calculated signal strengths by the values just calculated; i.e., add 500 of the values calculated in Section 5.9.2.3 to the proposed station value calculated in Section 5.9.2.1, add the next 500 to the first interferer's value, etc. Note that, since the values calculated in Section 5.9.2.3 will have both positive and negative values, the results of Section 5.9.2.3 will sometimes be larger and sometimes smaller than Section 5.9.2.1.

5.9.2.5 Calculations for Each of the Samples

For each of the (500) samples, convert the values for the potential interferers to absolute (not dB) values, sum them, and convert the sum back to dB. Subtract this value from the

value for the corresponding draw for the desired signal. If this number equals or exceeds the C/(I+N) goal, it is a "pass". Otherwise, it is a "fail".

5.9.2.6 Determine the Probability of a "Pass"

To determine the probability of a "pass" at a given location, divide the number of "passes" by the total number of samples (in the example, 500).

6.0 Performance Confirmation

This section addresses the issues associated with the empirical validation and quantification of wireless communications system performance. This process may be integral to a proof-of-performance or acceptance test or to quantify the actual interference environment versus simulated predictions in interference limited systems.

Conformance testing will validate that the user can expect to obtain the design reliability over their service area by measuring at a statistically significant number of random test locations, uniformly distributed throughout the service area. The entire concept of conformance testing rests on statistics.

The semantics of some of the terms used is critical to properly understanding this methodology. The service area is divided by a grid pattern to produce a large number of uniformly sized tiles, or test tiles. In one method, within each test tile a test location is randomly selected. At each of these test locations, a series of sequential measurements (**subsamples**) is made. This test location measurement, containing a number of subsamples, constitutes the **test sample** for this location.

Alternatively, the grid pattern is used to develop a test route that is uniformly distributed throughout the service area with an approximately equal distance traveled in each grid. This test route shall pass once through each test tile while collecting data. Thus, a large number of test samples is collected and evenly distributed throughout the service area.

6.1 Service Area Reliability

The service area reliability shall be determined by the requisite percentage of the test locations that meet or exceed the CPC.

$$\text{Service Area Reliability (\%)} = \frac{T_p}{T_t} \bullet 100\% \qquad \text{[Eq. 50]}$$

where:

T_p = Total of tests passed
T_t = Total number of tests

6.2 Determination of Number of Test Tiles

The "estimate of proportions" shall be used to determine with a high degree of confidence that sufficient test grids have been developed to accurately determine the Area Reliability.

6.2.1 Estimate of Proportions

$$T_1 = \frac{Z^2 \bullet p \bullet q}{e^2}. \qquad \text{[Eq. 51]}$$

where:

T_l = Number of Test Locations
Z = Standard Deviate Unit (Corresponding to the confidence level)
p = True Service Area Reliability (decimal)
$q = 1 - p$
r = Service Area Reliability Criterion (decimal)
e = Sampling error allowance (decimal)

This is subject to a limit such that :

$$T_l \geq 100 \qquad \text{[Eq. 52]}$$

The requirement is that T_l be the larger of the two values..

Values for the standard deviate are available in most statistics books. Some standard values for one sided (tail) tests [Z_α] and two sided (tails) tests [$Z_{\alpha/2}$] are shown in Table 13 of Appendix-A.

6.3 Pass/Fail Test Criteria

The following pass/fail criteria are possible:

- The "Greater Than" Test
- The "Acceptance Window" Test.

6.3.1 The "Greater Than" Test

The "Greater Than" Test requires that the percentage of test locations which meet the CPC must equal or exceed the service area reliability requirement. This necessitates a slight "overdesign" of the system by e% to provide the statistical margins for passing the conformance test as defined. For this test configuration, Z has one-tail [Z_α] and e is the decimal percentage of overdesign.

6.3.2 The "Acceptance Window" Test

The "Acceptance Window" test allows the percentage of test locations which meet the CPC to fall within an error window, $\pm e$, which is centered on the service area reliability requirement to consider the acceptance test a pass. This eliminates the requirement for "overdesign", but necessitates a two tail Z [$Z_{\alpha/2}$] which increases the number of test samples to be evaluated.

6.4 Confidence

6.4.1 Confidence Level

The greater the number of test locations, the higher the confidence level. The confidence level should reflect a high confidence that the measured values will indicate what the true value is. A confidence level of 99% should be used unless this choice forces the size of the test grids for the desired service area to become too small; i.e., $< 100\lambda$.

6.4.2 Confidence Interval

This defines the limits within which the true value should fall. Using the preceding example of an acceptance window test with a 99% confidence level and 2% error and a service area reliability requirement of 95%, the statement would be, "I am 99% confident that the true value lies between 93 and 97%".

6.4.3 Size Constraints

Test grid tiles (areas) should be $\geq 100\lambda$ by 100λ, but less than 2 km by 2 km. All test grids shall be of equivalent shape and area. A reasonable aspect ratio of 3:2 through 2:3 is considered to be square for the purpose of sizing test grid tiles of that shape. A tile created using other shapes, such as triangles and hexagons of equivalent areas is an acceptable alternative to a rectangularly shaped tile.

6.4.4 Accessibility

Locations with inaccessible test grids shall be specified, prior to testing, and treated per one of the following options:

- Eliminated from the calculation
- Considered a pass
- Estimated based on adjacent grids (single grids only)

6.5 Measurements

6.5.1 Carrier Power

The local mean power shall be measured with a receiver calibrated at its antenna port. See Section 6.8.3. The use of a mean power value requires a linear or logarithmic transfer function. Alternatively, if the transfer function of the detection system is known, but is non-linear, a suitable set of correction factors may be developed and applied to correct the non-linear ranges of the transfer function.

Other distributions may be captured and used for additional analysis of fading.

6.5.2 Distance

The distance (D) for measurements of the carrier local mean in a test grid shall be:

$29\ell \leq D \leq 100\ell$. The preferred distance is 40ℓ as it smoothes out Rayleigh fading. Shorter distances have a large impact from the Rayleigh fading. Larger distances tend to include changes in the local value due to the location variability starting to change. At lower frequencies, less than 40λ may be necessary.

Bit Error measurements may require longer distances and/or time intervals to capture the required number of test sub samples. It is recommended that separate local 40 λ values be captured so that failures can be analyzed.

6.5.3 Bit Error Rate

BER shall be measured using a suitable pseudorandom test pattern, e.g., the ITU-T V.52 or O.153 patterns. See Section 6.6.1.3.

6.5.4 Number of Subsamples Per Test Sample

The number of subsamples taken for each test sample to measure the mean or median power at each location shall be greater than 50. This is to produce a 90% confidence interval that the measured value is within ±1 dB of the actual value. To calculate different confidence intervals, use the following formulas, where T_s is the number of sub sample data points taken:

$$\text{90\% Confidence Interval (dB)} = 20Log\left(1+\left(\frac{1.65}{\sqrt{T_s}}\bullet\sqrt{\frac{4-\pi}{\pi}}\right)\right) \qquad \text{[Eq. 53]}$$

$$\text{95\% Confidence Interval (dB)} = 20Log\left(1+\left(\frac{1.96}{\sqrt{T_s}}\bullet\sqrt{\frac{4-\pi}{\pi}}\right)\right) \qquad \text{[Eq. 54]}$$

$$\text{99\% Confidence Interval (dB)} = 20Log\left(1+\frac{2.58}{\sqrt{T_s}}\bullet\sqrt{\frac{4-\pi}{\pi}}\right) \qquad \text{[Eq. 55]}$$

6.6 Adjacent Channel Transmitter Interference Assessment

A copy of the normalized power-density spectrum table is obtained for each adjacent channel transmitter within approximately 297 km (180 miles) of the station, and ± 25 kHz of the channel being coordinated. Each power-density value in the table is subsequently multiplied by the ERP of its respective transmitter, and each frequency value is shifted by an amount equal to the difference between the channel being coordinated and the assigned channel frequency of the transmitter being assessed. Further, the power density table is scaled by the amount of attenuation associated with the station separation in accordance with the standard propagation model described in Section 5. (Note: subsequent paragraphs 6.6.1.1 and 6.6.1.2 explain how a power-density spectrum table may be generated from transmitter measurements.)

In addition, a normalized receiver selectivity characteristic table is obtained for the receivers to be used on the channel being coordinated. The adjacent channel coupled power (ACCP) from each transmitter is then determined by multiplying the adjacent channel transmitter table described

above with the receiver table over the bandwidth of the receiver. The ACCP from all adjacent channel transmitters is then summed to give the total receiver ACCP.

In Appendix C, Tables C-1 and C-2 contain a coarse table for 11K0F3 and 16K0F3 modulation. Tables C-3 through C-9 contain the calculated ACCP for some of the common IF configurations. The amount of power intercepted by the stated IF is shown for the VHF and UHF bands with the normal spacing and split channel spacings. Three analog configurations are shown that are varied for the transmitter low pass filter appropriate for the band. For VHF it is a 2 pole filter; for UHF is a 3 pole filter; and for narrowband FM it is a 5 pole filter. For analog FM (e.g., 20K0F3E) a standard TIA 603 receiver shall be assumed unless noted otherwise.

The total ACCP is added to the IF noise power as determined in Section 3.6.3 to result in the level of interference plus noise power to be overcome by the received power of the desired signal. The received power of the desired signal is determined by using the propagation model and the ERP of the desired transmitter.

The desired signal power is numerically divided by the interference power to determine the system signal to interference plus noise ratio, and converted to dB. If the resulting value is greater than the value necessary for the desired channel performance criterion (CPC) for the given technology according to Table 5, the result is said to be a "pass"; otherwise the result is said to be a failure.

6.6.1 Normalized Power-density Spectrum Table

A transmitter's emissions may be characterized by a measurement of its power-density spectrum over a specified frequency span using an adjacent channel power (ACP) analyzer or a spectrum analyzer. This type of analyzer typically presents the emission spectrum using an oscilloscopic display of a locus of 501 to 1001 discrete data points, each data point representing the amount of power measured in a "frequency bin". The frequency "sweep" is accomplished by incrementing the measurement frequency one step at a time at a value determined by the span setting.

The measured values are properly compensated by the analyzer for the characteristics of the filter used for the measurement. A table of the amplitude and frequency of each data point may then be obtained via the analyzer bus, or a floppy disk interface, and subsequently formatted into a computer file which may be used for assessment analysis. This file can be normalized by determining the power-density in each "frequency bin" of the measured span relative to the total power of the emission, and making the center frequency equal to zero.

To measure both on-channel and adjacent channel power it is necessary that the frequency span of the measurement be at least 3 times the channel spacing.

To facilitate assessment computations, it is desirable to have only one value of frequency step, and it must not exceed the resolution bandwidth. Since there is a 2:1 range in the frequency step size used between manufacturers and models of currently available analyzers, but most have an adjustable span, then a power-density spectrum table with a uniform step size may be obtained by

setting the span to equal N-1 times the step size as shown in Table 8 of Appendix-A. Table 8 lists the frequency span and resolution bandwidth to use for the various channel spacings that will be encountered.

It is recognized that the trace data output sequence, data retrieval and analyzer bus control commands, and floppy disk formats (not universally available at this time) differ between the various spectrum analyzer vendors so the captured transmitter power-density spectrum data table may need to be converted into the table format needed for performing the interference analysis via a floppy disk or Internet data transfer means.

6.6.1.1 Power-density Spectrum Table for an Analog Modulated Transmitter

1. Connect the equipment as illustrated in the following diagram, with the transmitter set to produce rated RF at the assigned frequency, and the signal analyzer set to use average power detection and the span and resolution bandwidth given in Table 8. (Note that the audio mixer may be eliminated if the audio generators are series connected.)

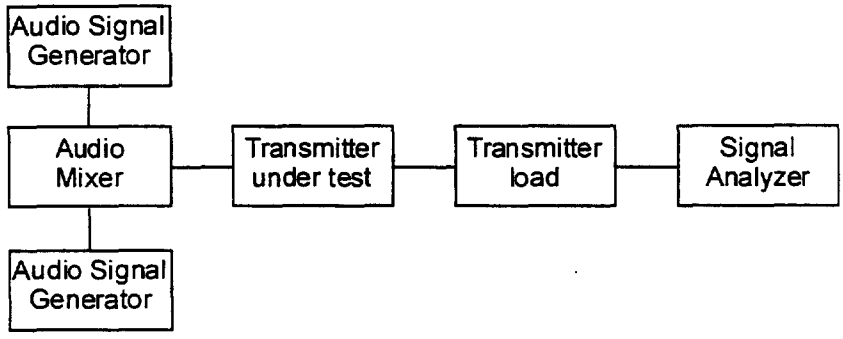

Figure 10. Two Tone Modulation Setup

2. Adjust the frequency of one audio generator to the lower frequency of the frequency pair given in Table 7 of Appendix-A for the modulation technology under test.

3. With the other audio generator off, modulate the transmitter with the low frequency audio tone only and adjust the generator output voltage to produce 50% of rated modulation. Record this level, then reduce the low frequency tone level by at least 40 dB.

4. Turn on the other audio signal generator and set its frequency to modulate the transmitter with the higher frequency tone of the frequency pair.. Adjust the generator output voltage to produce 50% of rated modulation and record this level.

5. Increase the output level of each signal generator respectively to a level 10 dB greater than the levels recorded in steps 3 and 4.

6. Capture the emission on the signal analyzer using a span no less than the appropriate span listed in Table 8. Generate a power-density spectrum table by recording the center

frequency of, and the power in, each frequency bin of the spectrum produced by the emission.

7. Sum (linearly, not using logarithms) the power values in each bin of the spectrum produced by the signal analyzer, then record this total power value as the transmitter power.

8. Normalize the table by dividing the power value in each bin by the total power recorded in step 7, and setting the center frequency of the spectrum to 0 Hz. This is the normalized power-density spectrum table.

6.6.1.2 Power-density Spectrum Table for a Digitally Modulated Transmitter

1. Connect the equipment as illustrated below with the transmitter set to produce rated RF power at the assigned frequency, and the signal analyzer set to use average power detection with a span and resolution bandwidth per Table 8.

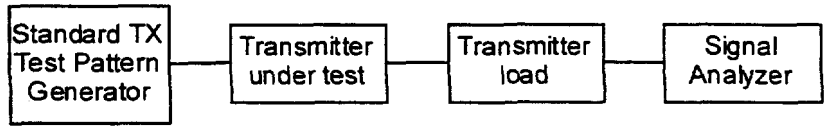

Figure 11. Digital Modulation Measurement Setup

2. Set the test pattern generator to produce the test pattern given in Table 7 of Appendix-A at the normal modulation level plus the maximum operating variance for the modulation technology under test.

3. Capture the emission on the signal analyzer using a display span no less than the appropriate value listed in Table 8. Generate a power-density spectrum table by recording the center frequency of, and the power in, each frequency bin of the spectrum produced by the emission.

4. Sum (linearly, not using logarithms) the power values in each bin of the spectrum produced by the signal analyzer, then record this total power value as the transmitter power.

5. Normalize the table by dividing the power value in each bin by the total power recorded in step 4), and setting the center frequency of the spectrum to 0 Hz. This is the normalized power-density spectrum table.

6.6.1.3 Digital Test Pattern Generation

The digital test patterns are based on the ITU-T V.52 pseudo-random sequence. The FORTRAN procedure given below generates this pattern for binary and four level signals.